Journal of Alloys and Compounds, 213/214 (1994) 20–27
JALCOM 4017

Chemistry of the transactinide elements

J.V. Kratz
Institut für Kernchemie, Universität Mainz, Fritz-Strassmann-Weg 2, D-55099 Mainz (Germany)

Abstract

Some of the challenges involved in the study of the short-lived isotopes of the transactinides which can only be produced an "atom-at-a-time" are considered, and the types of experiments are discussed. Elements 104 and 105 behave as members of groups 4 and 5, as expected. However, deviations of the chemical properties from expectations based on simple extrapolations have been observed: for example, the volatility of element 104 chlorides is intermediate between that of Zr and Hf chlorides, and the volatility of element 105 bromides is less than that of Nb and Ta bromides. In aqueous solution, at times, element 104 behaves more like Pu^{4+} than Zr^{4+} and Hf^{+}, and element 105 exhibits a non-Ta-like behaviour and similarity to Pa^{5+} and Nb^{5+}. Relativistic molecular calculations are being performed in order to gain an understanding of this complex chemistry.

1. Introduction

After the pioneering studies of some basic chemical properties of the early transactinide elements 104 and 105 in the 1970s (see refs. 1–4 for complete reviews) that confirmed the placement of these elements in groups 4 and 5 of the periodic system, there is renewed interest in studying in more detail the chemical properties of the transactinides [5, 6]. This is because computer-controlled automated systems have greatly enhanced our ability to perform rapidly and reproducibly the hundreds or sometimes thousands of successive separations required to obtain statistically significant results, and because relativistic quantum-chemical codes at the Dirac–Fock level are now becoming capable of modelling complex molecules. By comparison of the chemical behaviour of elements 104 and 105 with that of their lighter homologues Zr and Hf, and Nb and Ta, respectively and with some pseudohomologues in the light actinides, and by comparison of the details observed experimentally with results of relativistic molecular orbital (MO) calculations it is hoped to evaluate the role of "relativistic effects" in the chemistry of these very heavy elements.

In this paper, a review is given of the experimental techniques and results of both aqueous and gas phase studies of elements 104 and 105 and their homologues, and prospects for studies of still heavier elements are briefly considered. Because of space limitations, this review cannot be complete at all, and the following papers are referred to for further details.

2. Production, transport, and detection

Most of the chemical studies of elements 104 and 105 have used the isotopes 78-s $^{261}104$ produced in the $^{248}Cm(^{18}O, 5n)$ reaction with a cross-section of 5 nb and 34-s $^{262}105$ produced in the $^{249}Bk(^{18}O, 5n)$ reaction with a cross-section of 6 nb respectively. For a target thickness of 700 $\mu g\ cm^{-2}$, a collection time of 60 s, a beam current of 2.5 eμA of $^{18}O^{5+}$ ions, start of measurement 60 s after end of collection, and a measurement efficiency of about 0.5, one observes on the average one atom every 20 min, *e.g.* one atom in 20 successive 1 min collection and separation cycles. Thus, the experiments are truly performed with single atoms. The question of whether single-atom chemistry can give equilibrium constants that are close to the true value is discussed below. The target arrangement is schematically shown in Fig. 1. The beam of ^{18}O ions passes through a HAVAR™ vacuum isolation window, a volume of nitrogen cooling gas, and a Be target backing before interacting with the target material. The reaction products recoiling out of the target are stopped in a volume of He loaded with KCl or MoO_3 aerosols and transported through a polyethylene capillary to the collection site or to either one of the chemistry systems to be introduced below.

The single atoms of $^{261}104$ or $^{262}105$ are detected by α particle and spontaneous fission (SF) pulse height analyses using chemically inert passivated implanted planar silicon (PIPS) detectors. The pulse heights are digitized and stored in list mode on magnetic tape together with the time after start of counting and the

SSDI 0925-8388(93)04017-K

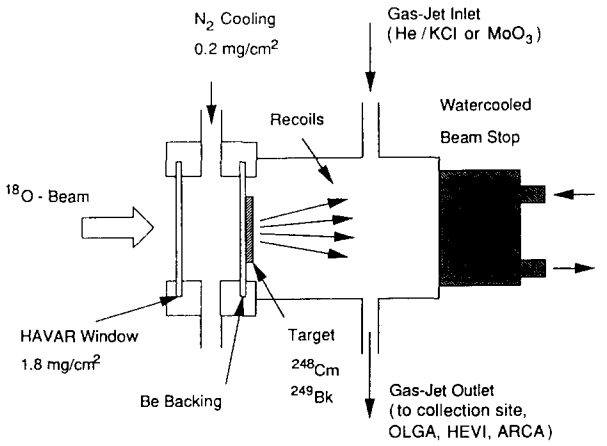

Fig. 1. Schematic representation of a target arrangement.

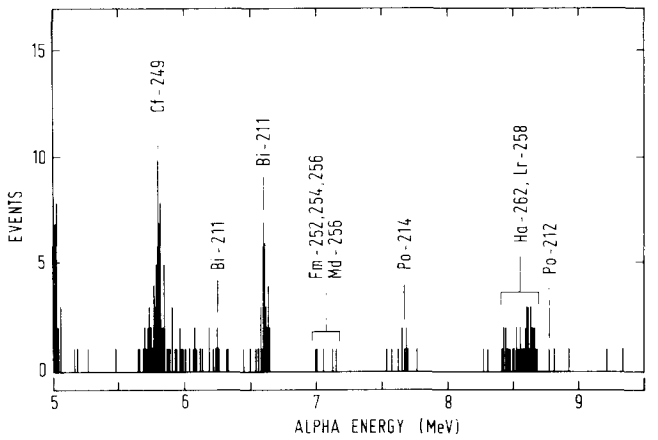

Fig. 2. α energy spectrum of element 105 fractions in the α-HiB chemistry (figure adapted from ref. 7). The results of 525 collection and elution cycles are summed up.

identification of the detector in which the event occurred. This list mode storage allows versatile off-line processing of the data, including searches for time-correlated parent–daughter pairs of α events in the same detector. An example for an α energy spectrum resulting from 525 collection and elution cycles (each of 1 min) of 34-s $^{262}105$ using cation exchange chromatography with aqueous solutions of α-hydroxyisobutyric acid (α-HiB) [7] in the automatic rapid chemistry apparatus (ARCA II) [8] is shown in Fig. 2. At a detection efficiency of 0.35 for a single α particle, the efficiency for detecting both mother and daughter α particles is $0.35 \times 0.35 = 0.12$. The 39 α singles attributable to the decay of $^{262}105$ and the daughter ^{258}Lr, which decays in transient equilibrium with its mother, give a half-life of $35.7^{+6.9}_{-5.4}$ s. In nine events, the decay of $^{262}105$ is followed shortly by a ^{258}Lr decay, giving a half-life of $4.2^{+1.5}_{-1.1}$ s for ^{258}Lr. These events are accompanied by 23 SF events. The α energies, the associated lifetimes (half-lives), the relative number of associated time-correlated pairs and SF decays provide a unique identification of the presence of $^{262}105$. The minor contaminants in the spectrum (^{249}Cf sputtered from the target, small residual Bi and Po activities produced by transfer reactions on a Pb impurity in the target, and a small residual Fm–Md activity from transfer reactions with the target, both the Bi–Po and the Fm–Md activities being depleted by many orders of magnitude by the chemical separation) do not interfere with the $^{262}105$–^{258}Lr activity in the indicated energy window. Thus, even single events in this energy window can be safely assigned to $^{262}105$–^{258}Lr.

3. Single-atom chemistry?

Given the possibility to produce, transport, and detect single atoms of the transactinide elements, the question arises as to whether a meaningful chemistry with single atoms is possible. A number of papers have addressed this basic question. Guillaumont *et al.* have pointed out that for single atoms the classical law of mass action is no longer valid [9] because the atom cannot exist in the different chemical forms taking part in the chemical equilibrium at the same time. Guillaumont *et al.* suggest for single-atom chemistry to introduce a specific thermodynamic function, the single-particle free enthalpy, or the expectation value thereof. Then, an expression equivalent to the law of mass action is derived in which concentrations (activities) are replaced by probabilities of finding the atom in a given state and in a given phase. According to this law, the distribution coefficient of the atom between two phases is correctly defined in terms of the total probabilities of finding the atom (whatever its species) in one phase or the other. If a static partition method is used, this coefficient must be measured in repetitive experiments. Since dynamical partition methods can be considered as spatially repetitive static partitions, the displacement of the atom, in itself, is a statistical result and only one experiment is necessary, in principle [9]. This underlines the validity of partition experiments with single atoms and the particular attractivity of chromatographic methods in single-atom chemistry.

Borg and Dienes [10] have considered the kinetics of a single-step exchange reaction $MX + Y \rightleftharpoons MY + X$ where M is a single metal ion and the displacement from left to right is associated with a free enthalpy ΔG^+ of activation. If ΔG^+ was less than about 15–17 kcal, the residence time of M in each state MX or MY was calculated to be very short and an equilibrium would be rapidly reached (in times short compared with the nuclear half-lives of $^{261}104$ or $^{262}105$). They found that, once equilibrium is reached, the fractional average time that M spends as MX or MY is proportional to the equilibrium constant. Thus, a measurement of

the partition of M between the states MX and MY with very few atoms of M will already yield an equilibrium constant close to the "true" value provided that both states are rapidly sampled. This tells us again that chromatographic systems are ideally suited for single-atom separations as there is rapid, multiple sampling of the absorbed or mobile species. Here, the fractional average time that M spends as the absorbed species or the mobile species (the equilibrium constant) is closely related to the chromatographic observable, the retention time.

4. Experimental techniques

Early gas phase separations of element 104 and 105 chlorides and bromides by Zvara *et al.* have mostly used the principle of thermochromatography in which a temperature gradient is applied along the chromatographic tube and the volatile species deposits at a particular position inside the tube corresponding to a given deposition temperature and adsorption enthalpy. The disadvantage of this approach is that real-time detection of the nuclear decay of the transactinides is not possible and the detection is limited to fission-track counting. Therefore, the more recent experiments conducted at Berkeley and Darmstadt have used isothermal gas chromatography in which the volatile species leave the column, and are reattached to new aerosol particles (N_2–KCl or Ar–KCl) for transport to the detection system [11]. Two versions, the on-line gas chromatography apparatus (OLGA II) and the technically improved heavy element volatility instrument (HEVI) were used. The experimental set-up is shown in Fig. 3. Both systems consisted of a quartz column (6 mm inner diameter) separated into two sections. The first one in which the aerosols were stopped on a quartz wool plug was kept at 900 °C to destroy the aerosols. KCl clusters were used in earlier work [12] with the disadvantage that KCl recondensed in the colder, isothermal part of the column and the chromatography probably took place on a KCl surface. Later [13], MoO_3 aerosols were used. These have the advantage that they form very volatile oxychlorides that do not deposit inside the chromatography column. At the position of the quartz wool plug reactive agents such as HBr, BBr_3, HCl or Cl_2 were added at a flow rate of about 100–200 ml min^{-1}. The second part of the column served as the isothermal chromatography section. Its temperature was varied between 50 °C and 800 °C in 50 °C intervals. Volatile halide species formed at the position of the quartz wool plug were then transported along the cooler chromatography section of the column by the He flow. One is determining the retention times of the volatile species by using the half-lives of the nuclides as a "clock". Reaction products leaving the column were reattached to new aerosols and detected either in a rotating wheel system [13] or on a moving tape system [12].

Recent aqueous phase chemistry studies of the transactinides were either performed by manual separations [14, 15] or with the automated high pressure liquid chromatography (HPLC) system ARCA II [8, 7, 16–18]. The separation procedure for manual TBP extraction studies of element 104, as an example, is as follows [15]. Collect activity from gas jet for 90 s; pick up activity with 10 μl of HCl–LiCl phase; add to 1 ml centrifuge cone containing 20 μl of TBP phase; mix ultrasonically; centrifuge; remove TBP phase and dry on a hot Al disc; place Al disc in counter. This procedure

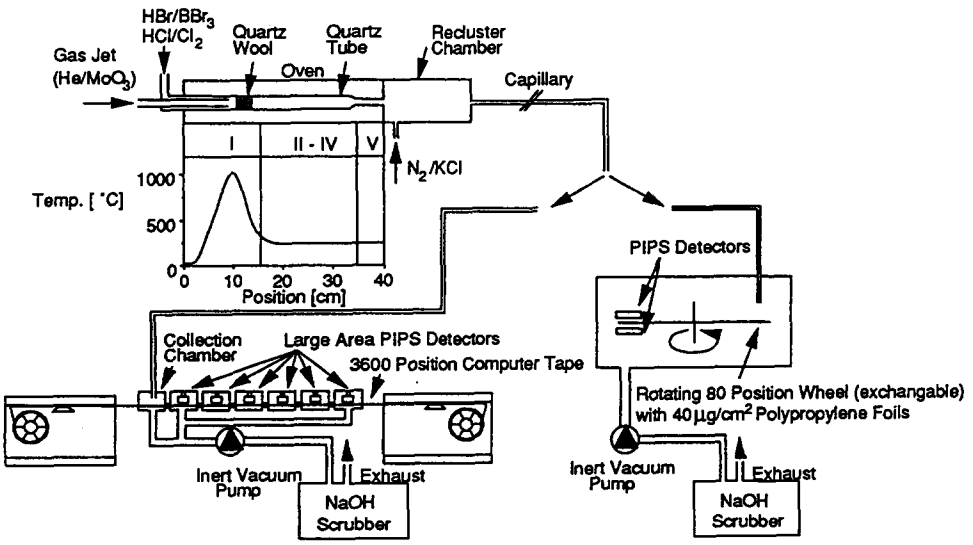

Fig. 3. Schematic of the isothermal gas chromatography systems (OLGA or HEVI) in combination with a wheel system to study volatile element 104 chlorides or with a tape system used to study volatile element 105 bromides [11].

takes about 1 min. Extraction studies of element 104 of this type have been conducted with TBP, TiOA, and TTA [15]. HPLC separations with ARCA II have focused on the study of the aqueous phase chemistry of element 105 using reversed-phase microchromatographic columns incorporating TiOA [16, 18] or DIBC [17] on an inert support. A schematic representation of the ARCA II components is given in Fig. 4. ARCA II consists of a central catcher–chemistry part incorporating the sliders SL1–SL3, and two movable magazines containing 20 of the chromatographic columns C1, C2 (1.6×8 mm) each, and of peripheral components, *i.e.* three chemically inert HPLC pumps, P1–P3, and a number of pneumatically driven four-way slider valves, S1–S4. All processes in ARCA II are controlled by a microcomputer. Each pump pumps one eluent, *e.g.* one 12 M HCl–0.02 M HF, another 4 M HCl–0.02 M HF, and the third 6 M HNO_3–0.015 M HF, through Teflon tubing of 0.3 mm inner diameter to the central catcher–chemistry unit. The He–KCl gas jet deposits the transported reaction products continuously onto one of two alternating polyethylene frits F. After 1 min collection, the first frit is moved on top of one of the microcolumns C1, washed with 12 M HCl–0.02 M HF, whereby the reaction products are dissolved, complexed, and extracted into the TiOA (in case of Nb, Ta, Pa, and element 105), while the non-extractable species (notably the actinides) run through into the waste, W3. The column is then washed with 4 M HCl–0.02 M HF, and the effluent (containing Nb, Pa, and element 105) is directed through SL2 to the fraction collector FC where it is collected on a Ta disc and quickly evaporated to dryness by intense IR light and hot He gas. Next, the Ta fraction is eluted in 6 M HNO_3–0.015 M HF, collected on a Ta disc, and evaporated to dryness. The Ta discs are inserted into the counting chambers about 55 s after the end of collection. 5 s later the next 1 min collection on the twin frit is complete. That frit is moved on top of the column C2 contained in the opposite magazine, and the next separation cycle is carried out. After each separation, the magazines are moved by one step, thus introducing a new column into the elution position. In this way, the time-consuming reconditioning of used columns is avoided. After 40 min of continuous collection and separation cycles the program is stopped, the used magazines are removed, two new magazines are introduced, and another 40 cycles are started. More than 6500 ARCA experiments have been conducted in the study of element 105 so far.

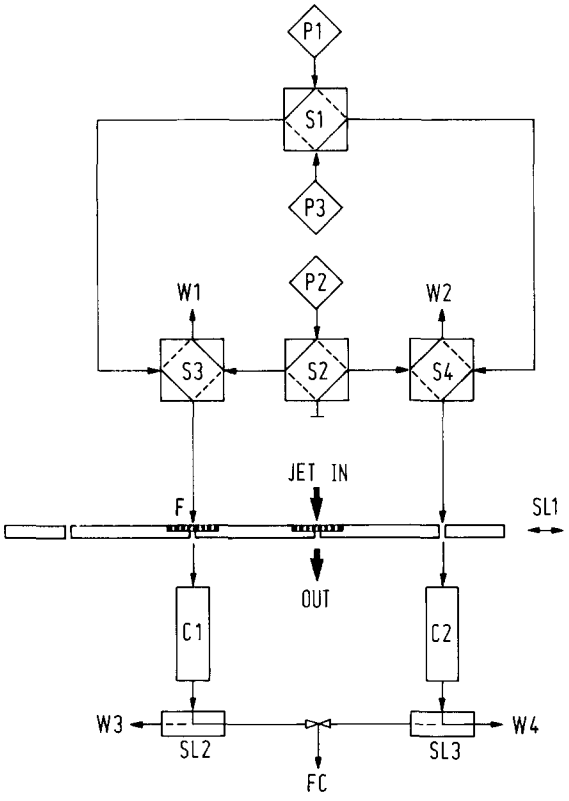

Fig. 4. Schematic of ARCA II [8].

5. Results

Figure 5(a) shows the chemical yield of volatilized element 104 chlorides as a function of the temperature of the isothermal section of the chromatography tube in comparison with the behaviour of the chlorides of ^{98}Zr and ^{162}Hf [13]. Also shown, in Fig. 5(b), is the chemical yield of element 105 bromides compared with the behaviour of ^{99g}Nb and ^{167}Ta [12]. The full lines are the results of Monte Carlo simulations [11] based on the microscopic model of gas–solid thermochromatography proposed by Zvara [19]. The simulation accommodates the influence of the carrier gas flow, the actual temperature profiles, and the different half-lives of the investigated species. For each isothermal temperature, the transport through the column is modelled for a large number of sample molecules. These calculations result in a curve of yield *vs.* temperature for each value of the absorption enthalpy ΔH_a. The curve for the particular ΔH_a value which best fits the measured data is chosen by a least-squares method. ΔH_a is essentially determined by the temperature value $T_{50\%}$ at the relative chemical yield of 50%. At this temperature, the retention time t_r is equal to the half-life of the nuclide [20]. In the correlation of t_r with ΔH_a a calculated value for the absorption entropy ΔS_a according to the formalism of Eichler and Zvara [21] is used.

The results for the group 4 chlorides have been interpreted so as to establish the following series in

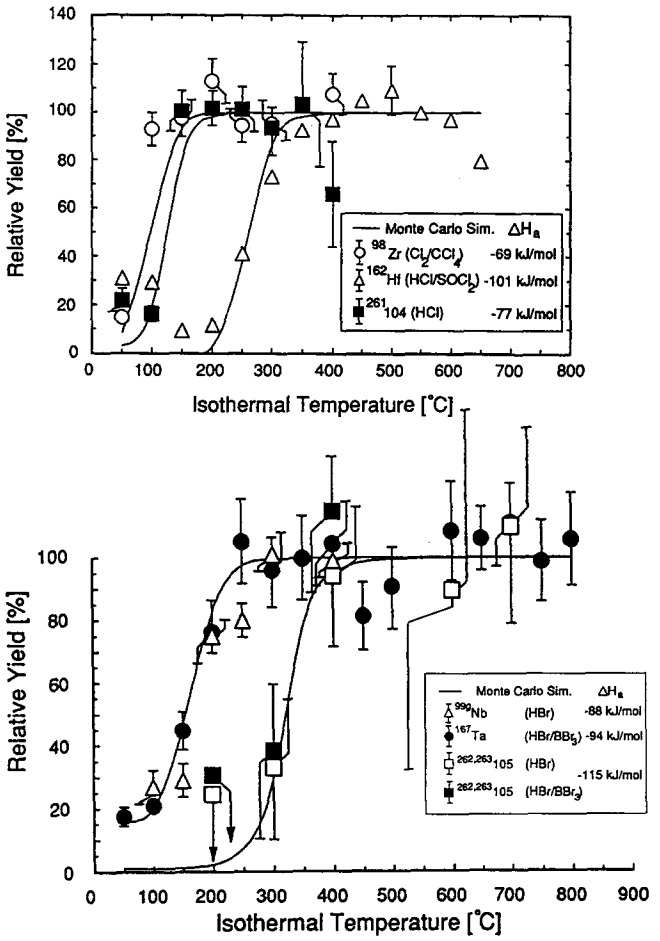

Fig. 5. Chemical yield *vs.* temperature for (a) the tetrachlorides of group 4 and (b) the pentabromides of group 5 [11].

volatility: Zr ≥ element 104 > Hf [11]. The higher value of ΔH_a for Hf was suggested to indicate that $HfOCl_2$ instead of the pure tetrachloride may have been studied. It is interesting to note that values of ΔH_a around -70 kJ mol^{-1} for Hf can also be found in the literature which are indicative of $HfCl_4$ being volatilized. Also, higher values of ΔH_a around -90 kJ mol^{-1} for Zr and element 104 indicative of the oxychlorides have been reported; see ref. 11. Thus, one must say that the chemical composition of the investigated species has not been governed decisively enough by the experiments performed until now. Further experiments under absolutely oxygen-free conditions are needed before any conclusions on the influence of relativistic effects on the volatility of element 104 halides can be drawn.

The results on the group 5 bromides [12], Fig. 5(b), seem to establish the following series in volatility: Nb ≥ Ta > element 105. This is in agreement with older and more recent thermochromatographic results by the Dubna group; see ref. 11. However, according to the results of relativistic molecular calculations by Pershina *et al.* [22], $105Br_5$ has the highest covalency and lowest effective charge which should make it more volatile than its homologues. Further experiments are needed to establish whether the volatilities measured are for $105OBr_3$ or $105Br_5$. Results on the volatility of element 105 chlorides are still preliminary but indicate a higher volatility than for the element 105 bromides.

As one of the highlights in the aqueous chemistry studies of element 104, Fig. 6 shows the distribution of $^{261}104$, ^{169}Hf, ^{228}Th, ^{95}Zr, and ^{238}Pu between an aqueous phase being 8 M in H^+ and a TBP phase as a function of the chloride concentration in the aqueous phase [15] (TBP extracts neutral complexes). Here, element 104 behaves differently from Hf^{4+} and Th^{4+}, and most like Pu^{4+}. The element 104 extraction reaches a maximum around 10 M Cl^- while the extraction of Hf^{4+} and Th^{4+} continues to increase. This indicates that element 104, unlike Hf^{4+} and Th^{4+}, forms anionic chloride species (which do not extract), similar to those of Pu^{4+} at higher Cl^- concentrations. Studies of element 104 extraction as a function of $[H^+]$ with $[Cl^-]$ constant at 12 M showed that extraction of element 104 increased sharply with $[H^+]$, a behaviour not exhibited by Zr and Hf [15]. The formation of $104Cl_5H \cdot x$TBP might be an explanation. The extraction of anionic complexes by TiOA shows element 104 to behave like Zr^{4+} and not like Th^{4+} [15]. The extraction of element 104 cations with TTA gives a distribution coefficient for element 104 between those of Th and Pu and indicates that the hydrolysis of element 104 is less than that for Zr, Hf, and Pu [15].

The first studies of the aqueous chemistry of element 105 [14] showed that element 105 adheres to glass surfaces on fuming with nitric acid as do Nb and Ta. However, from a mixture of HNO_3 and HF, element 105 could not be extracted into MIBK [14] under conditions in which Ta extracts but Nb does not. To investigate the unexpected behaviour of element 105 in more detail, ARCA separations were performed in which element 105 was found to sorb on TiOA columns from either 12 M HCl–0.02 M HF or 10 M HCl, as do Nb, Ta, and Pa [16]. Elution positions of element 105 relative to those of Nb, Ta, and Pa were determined in 10 M HCl–0.025 M HF, 4 M HCl–0.02 M HF, and 0.5 M HCl–0.01 M HF, and the results are indicated by the bold bars in Fig. 7 [16, 18]. At all HCl concentrations, element 105 is found to behave similarly to Nb and Pa, and to be very different from its closest homologue, Ta. The well-known differences in the complex chemistry of Nb and Ta that are the basis for their industrial separation are that Nb is known to form weaker complexes of the $[NbOX_4]^-$ type (X ≡ Cl, F) which are also known for Pa. These may be in hydrolysis equilibrium with $[Nb(OH)_2X_4]^-$. For Ta, stronger largely covalent complexes of the pure halide type such as $[TaX_6]^-$ are predominant. From the non-

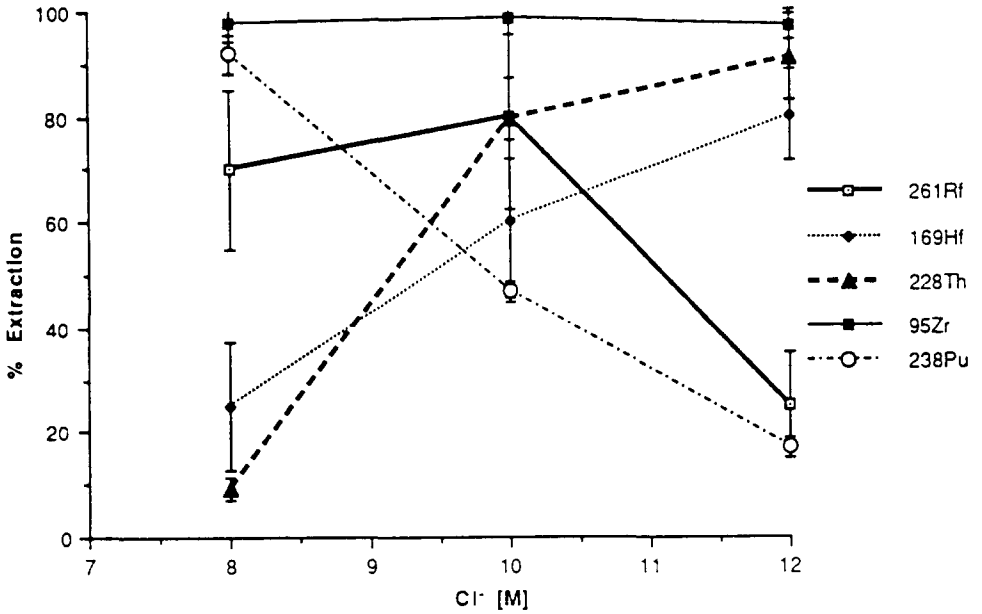

Fig. 6. Extraction of $^{261}104$, ^{169}Hf, ^{228}Th, ^{95}Zr, and ^{238}Pu into TBP *vs.* chloride concentration. The H^+ concentration is kept at 8 M. (From ref. 15.)

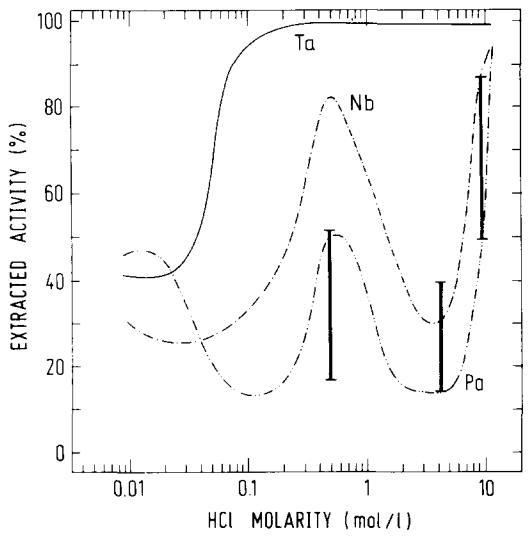

Fig. 7. Extracted activity of Ta, Nb and Pa *vs.* HCl molarity in the system TiOA–(HCl–HF). The bold bars encompass the upper and lower limits deduced from the element 105 elution positions (adapted from ref. 18).

Ta-like behaviour of element 105 and its similarity in the TiOA separations to Nb and Pa, the authors of refs. 16 and 18 concluded that the complex structures of element 105 must be of the Nb, Pa type. Elutions of element 105 from cation exchange columns in dilute unbuffered α-HiB solution provided an unambiguous proof that pentavalent element 105 is the most stable valence state in aqueous solution [7]. These very efficient separations were also instrumental in the discovery, at 93 MeV bombarding energy, of the $^{249}Bk(^{18}O, 4n)$ product $^{263}105$ [23]. Extractions of element 105, Nb, and Pa from strong HBr solutions into DIBC [17] showed that the tendency to form polynegative anions is in the sequence Pa < Nb < element 105.

6. Element 106 and beyond

It appears possible with existing technology to extend our studies of the transactinides to element 106, in particular since there is evidence from Dubna for the presumably longer-lived (than 0.9-s $^{263}106$) isotopes $^{265}106$ and $^{266}106$ produced in the $^{248}Cm(^{22}Ne, 4, 5n)$ reactions [24]. ARCA separations based on chloride–fluoride complexation, liquid–liquid extractions using SISAK 3 in connection with liquid scintillation counting, and gas chromatography of the oxychlorides ($MO_2Cl_2(g)$) or acids ($H_2MO_4(g)$) have been tested with Mo and W, and related poster presentations are given at this conference. The prospects of going beyond element 106 depend on whether longer-lived species of these elements can be synthesized; see discussion in ref. 6.

7. Quantum chemical calculations

The status of relativistic atomic orbital and MO calculations whose results need to be compared with the experimental results in order to elucidate the role of relativistic effects in the chemistry of the transactinides is reviewed by V. Pershina at this conference.

Often, such comparisons have to involve a good deal of additional physicochemical consideration because the "observables" in the results of quantum chemistry are not the same as the experimental observables. Here, reference is made to a few calculations only for which a direct correlation of the results with experimental observations was possible. Zhuikov *et al.* [25] performed calculations of the electronic structure of MCl_4 (M ≡ Zr, Hf, and element 104) with the self-consistent field X_α scattering wave Dirac–Slater method and found a lower effective charge of element 104 compared with Zr and Hf. This low effective charge was predicted to cause a higher volatility of $104Cl_4$ compared with $ZrCl_4$ and $HfCl_4$. The experimental verification of this effect will require very careful high-resolution isothermal chromatography. Pershina *et al.*, by using the Dirac–Slater discrete variational method (DS-DVM), have investigated the overlap population data (which are a measure of the degree of covalency of the bonds) and the effective charges for MBr_5 (M ≡ Nb, Ta, Pa, and element 105) [22]. The lowest effective charge and the highest covalency should make $105Br_5$ the most volatile species among its homologues. An experimental verification, also here, will depend on improved experiments. In order to see whether the different complex structures of Nb and Pa on the one side and of Ta on the other side correlate with results of quantum chemical calculations, Pershina *et al.* [26] performed DSDVM calculations on the pure halides $[MCl_6]^-$ and on $[MOCl_4]^-$ and $[MOCl_5]^{2-}$ respectively, with M ≡ Nb, Ta, element 105, Pa. For the pure halide complexes, the Ta complex exhibits the highest total overlap population, considerably higher than for the corresponding oxygen-containing Ta complex. According to the overlap populations, Nb has equal trends to form pure halide or oxyhalide species. Pa has a slight preference for $[PaOCl_5]^{2-}$, and the strongest tendency to form the oxyhalide complex is predicted for element 105. The oxygen-containing complexes have higher effective charges and carry dipole moments, both contributing to a lower extractability of these ions into the organic phase as compared to the largely covalent (hydrophobic) $[TaCl_6]^-$. It is very gratifying to see that this analysis gives results that are consistent with the experimental observations. This example gives hope that further comparisons of this type will increase our understanding of the sometimes surprising chemical properties of the transactinide elements.

Acknowledgment

This work was sponsored by the German Minister for Science and Technology (BMFT) under Contract 03HE2MAI.

References

1 O.L. Keller and G.T. Seaborg, *Annu. Rev. Nucl. Sci., 27* (1977) 139.
2 E.K. Hulet, in N.M. Edelstein (ed.), *Actinides in Perspective, Proc. Actinides 1981 Conf.,* Pergamon, Oxford, 1982, p. 453.
3 O.L. Keller, *Radiochim. Acta, 37* (1984) 169.
4 R.J. Silva, in J.J. Katz, G.T. Seaborg and L.R. Morss (eds.), *The Chemistry of the Actinide Elements,* Chapman and Hall, London, 2nd edn., 1986, p. 1103.
5 M. Schädel, *6th Int. Conf. on Nuclei Far From Stability and 9th Int. Conf. on Atomic Masses and Fundamental Constants, Bernkastel-Kues, 1992,* in *Inst. Phys. Conf. Ser. 132* (Sect. 4) (1993) 413.
6 D.C. Hoffman, *Robert A. Welch Foundation Conf. on Chemical Research XXXIV, Fifty Years With Transuranium Elements, Houston, TX, 1990,* Lawrence Berkeley Laboratory Rep. LBL-29815, 1990.
7 M. Schädel, W. Brüchle, E. Schimpf, H.P. Zimmermann, M.K. Gober, J.V. Kratz, N. Trautmann, H. Gäggeler, D. Jost, J. Kovacs, U.W. Scherer, A. Weber, K.E. Gregorich, A. Türler, K.R. Czerwinski, N.J. Hannink, B. Kadkhodayan, D.M. Lee, M.J. Nurmia and D.C. Hoffman, *Radiochim. Acta, 57* (1992) 85.
8 M. Schädel, W. Brüchle, E. Jäger, E. Schimpf, J.V. Kratz, U.W. Scherer and H.P. Zimmermann, *Radiochim. Acta, 48* (1989) 171.
9 R. Guillaumont, J.P. Adloff and A. Peneloux, *Radiochim. Acta, 46* (1989) 169.
10 R.J. Borg and G.J. Dienes, *J. Inorg. Nucl. Chem., 43* (1981) 1129.
11 A. Türler, H.W. Gäggeler, B. Eichler, D.T. Jost, J. Kovacs, U.W. Scherer, B. Kadkhodayan, K.E. Gregorich, D.C. Hoffman, S.A. Kreek, D.M. Lee, M. Schädel, W. Brüchle, E. Schimpf and J.V. Kratz, *Paul Scherrer Institut Rep. PSI-PR-93-12,* 1993.
12 H.W. Gäggeler, D.T. Jost, J. Kovacs, U.W. Scherer, A. Weber, D. Vermeulen, A. Türler, K.E. Gregorich, R.A. Henderson, K.R. Czerwinski, B. Kadkhodayan, D.M. Lee, M. Nurmia, D.C. Hoffman, J.V. Kratz, M.K. Gober, H.P. Zimmermann, M. Schädel, W. Brüchle, E. Schimpf and I. Zvara, *Radiochim. Acta, 57* (1992) 93.
13 B. Kadkhodayan, *Ph.D. Thesis, Lawrence Berkeley Laboratory Rep. LBL-33961,* 1993.
14 K.E. Gregorich, R.A. Henderson, D.M. Lee, M.J. Nurmia, R.M. Chasteler, H.L. Hall, D.A. Bennett, C.M. Gannett, R.B. Chadwick, J.D. Leyba and D.C. Hoffman, *Radiochim. Acta, 43* (1988) 223.
15 K.R. Czerwinski, *Ph.D. Thesis, Lawrence Berkeley Laboratory Rep. LBL-32233,* 1992.
16 J.V. Kratz, H.P. Zimmermann, U.W. Scherer, M. Schädel, W. Brüchle, K.E. Gregorich, C.M. Gannett, H.L. Hall, R.A. Henderson, D.M. Lee, J.D. Leyba, M.J. Nurmia, D.C. Hoffman, H. Gäggeler, D. Jost, U. Baltensperger, Ya Nai-Qi, A. Türler and Ch. Lienert, *Radiochim. Acta, 48* (1989) 121.
17 M.K. Gober, J.V. Kratz, H.P. Zimmernann, M. Schädel, W. Brüchle, E. Schimpf, K.E. Gregorich, A. Türler, N.J. Hannink, K.R. Czerwinski, B. Kadkhodayan, D.M. Lee, M.J. Nurmia, D.C. Hoffman, H. Gäggeler, D. Jost, J. Kovacs, U.W. Scherer and A. Weber, *Radiochim. Acta, 57* (1992) 77.
18 H.P. Zimmermann, M.K. Gober, J.V. Kratz, M. Schädel, W. Brüchle, E. Schimpf, K.E. Gregorich, A. Türler, K.R. Czerwinski, N.J. Hannink, B. Kadkhodayan, D.M. Lee, M.J. Nurmia, D.C. Hoffman, H. Gäggeler, D. Jost, J. Kovacs, U.W. Scherer and A. Weber, *Radiochim. Acta, 60* (1993) 11.

19 I. Zvara, *Radiochim. Acta, 38* (1985) 95.
20 H. Gäggeler, H. Dornhöfer, W.D. Schmidt-Ott, N. Greulich and B. Eichler, *Radiochim. Acta, 38* (1985) 103.
21 B. Eichler and I. Zvara, *Radiochim. Acta, 30* (1982) 233.
22 V. Pershina, W.D. Sepp, B. Fricke, D. Kolb, M. Schädel and G.V. Ionova, *J. Chem. Phys., 97* (1992) 1116.
23 J.V. Kratz, M.K. Gober, H.P. Zimmermann, M. Schädel, W. Brüchle, E. Schimpf, K.E. Gregorich, A. Türler, N.J. Hannink, K.R. Czerwinski, B. Kadkhodayan, D.M. Lee, M.J. Nurmia, D.C. Hoffman, H. Gäggeler, D. Jost, J. Kovacs, U.W. Scherer and A. Weber, *Phys. Rev. C, 45* (1992) 1064.
24 R.W. Lougheed, personal communication, 1993.
25 B.L. Zhuikov, V.A. Glebov, V.S. Nefedov and I. Zvara, *J. Radioanal. Nucl. Chem., 143* (1990) 103.
26 V. Pershina, B. Fricke, J.V. Kratz and G.V. Ionova, submitted to *Radiochim. Acta.*